Tuning the magnetic moments in zigzag graphene nanoribbons: Effects of metal substrates

Jingzhe Chen,[1,*] Marco Vanin,[2] Yibin Hu,[1] and Hong Guo[1]

[1]*Centre for the Physics of Materials and Department of Physics, McGill University, Montreal, PQ, Canada H3A 2T8*

[2]*Center for Atomic-scale Materials Design, Department of Physics, Technical University of Denmark, DK-2800 Kgs. Lyngby, Denmark*

(Received 29 June 2012; published 27 August 2012)

We report a systematic theoretical investigation of the effects of metal substrates on the local magnetic moments of zigzag graphene nanoribbons (ZGNRs). Representative metal surfaces of Au, Pt, Ni, Cu, Al, Ag, and Pd have been analyzed from atomic first principles. Results show that the local magnetic moments vanish when the nanoribbons are on top of the surfaces of Al, Ag, Pt, and Pd, while they are preserved for Au, Ni, and Cu. For s-dominated metals, the magnetic moments of the edge states of ZGNRs can be tuned by a bias voltage. For p- or d-dominated metals there is significant hybridization between the metal states and the nonbonding π orbital of the ZGNRs; thereby the tuning effect is reduced. We identify the microscopic physical reason behind the bias tuning of the magnetic properties of the ZGNRs.

DOI: 10.1103/PhysRevB.86.075146 PACS number(s): 73.22.−f, 73.20.At, 73.20.−r, 73.40.Ns

I. INTRODUCTION

Graphene offers an interesting potential as an emerging material for electronics applications due to its unique properties. When a graphene sheet is narrowed down to a nanoribbon several nanometers wide, additional interesting phenomena occur since the edges come into play and contribute to the electronic structure.[1,2] The edge effects on the band structure of graphene nanoribbons (GNRs) depend on the atomic configurations at the edge. For zigzag-edge GNRs (ZGNRs), the localized nonbonding π states form a flat band at the Fermi level, giving rise to a high density of states (DOS); while for the armchair-edge GNRs, edge states do not exist thus producing a semiconducting ground state.[3,4] Interestingly, the edge states of the ZGNR are spin polarized, which has been theoretically predicted[5] and experimentally observed.[6] Since the magnetic edge states are spatially localized at the edges, they can be utilized as separate spin channels for spin-polarized quantum transport.[7–12] Furthermore, such spin channels can be switched on and off by tuning the magnetic moments of the ZGNR through external gates, which is proposed in several theoretical works.[13–16]

So far, most theoretical investigations have been on freestanding ZGNRs. Since graphene is often grown on metal substrates, the chemical interaction between the ZGNR and metal surface is an important and realistic experimental factor that should be carefully investigated. It is the purpose of this work to carry out a systematic theoretical investigation of the effects of metal substrates on the local magnetic moments (MMs) of ZGNRs. The local MMs of ZGNRs originate from the half-filled dangling bond of the edge atom which results in a sharp peak of DOS at the Fermi level. Due to the Stoner instability, this peak splits into two around the Fermi level thereby producing an antiferromagnetic ground state in the freestanding ZGNR. The existence of a metal substrate may significantly change this situation. Here we investigate the ground state atomic structures of a single-layer ZGNR on the fcc (111) surfaces of Ag, Al, Au, Cu, Ni, Pd, and Pt. The first-principles calculation results show that the interaction between the ZGNR and the metal surface can be classified into two groups. The first is the electrostatic interaction generated by the s-dominated metals such as Cu, Ag, and Au. The second is weak chemical interaction coming from the hybridization between the nonbonding π orbital in the ZGNR and the p or d states of the metal surface near the Fermi level, as in the cases of Al, Ni, Pd, and Pt. The energy spectrum of the ZGNR is shifted in the former group while distorted in the latter group. Importantly, for s-dominated metals the MMs can be tuned by an external bias voltage regardless of the initial state. However, such tuning does not work for the p- or d-metal surfaces.

The rest of the paper is organized as follows. In Sec. II, the relaxed atomic structures under the influence of metal substrate (at zero bias) are presented. The results at finite bias are shown in Sec. III, including the detailed partial density of states (PDOS) and charge transfer analysis. In Sec. IV, we discuss the calculation details and Sec. V is reserved for a brief conclusion.

II. RELAXED ATOMIC STRUCTURES

The relaxed atomic structures are found to be similar for all the metal substrates. As an example, Fig. 1 shows the top view and side view of the relaxed ZGNR/Au system. We model the metal substrate as a fcc (111) surface with the ZGNR aligned along the y direction. An intermediate lattice constant is used over the x-y plane in order to match the periodicities of both the metal and the ZGNR. A narrow ZGNR ($n = 4$) is picked because the gap originating from the edge states is inversely proportional to the width,[17] and also because a wider ZGNR on a wider metal substrate requires very large computational cost. Since the edge states are localized, the narrowness of the ZGNR will not affect the overall conclusions. As shown in Fig. 1(b), a counter electrode separated by a large vacuum is put on the far right of the ZGNR so that a bias potential can be applied across the ZGNR between the metal substrate and the counter electrode. The vacuum between the ZGNR and the counter electrode is fixed to about 10 Å that ensures no significant tunneling across the vacuum when a bias voltage is applied.

We use the grid mode of the density functional theory (DFT) package GPAW[18] for the structural relaxation where the electron wave functions are expanded onto a real-space grid to bypass the limitations of finite cutoff of the atomic orbital when

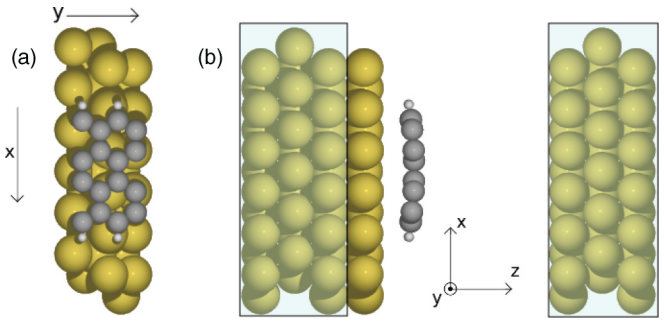

FIG. 1. (Color online) The relaxed atomic structure of a sample in the calculations, i.e., a zigzag graphene nanoribbon ($n = 4$) on the Au fcc (111) surface. (a) The top view of the system which is periodic along the x and y directions. (b) The side view. The regions in shadow are part of electrodes which extend periodically to $z = \pm\infty$.

describing the surface contact. The Perdew-Burke-Ernzerhof (PBE)[19] functional was employed. Reference 20 has shown that structures obtained by the local density approximation (LDA) for metal/graphene systems are in better agreement with experiments. However, PBE predicts more accurate binding energies in the case of ribbons where the binding originates from the edges and hence is more appropriate here. We use the standard DFT Hamiltonian without taking spin-orbit interaction into account. A (2,4,1) K-point sampling is adopted for all the calculations.

In Table I we list the relaxed distances of the ZGNRs from the different metal surfaces and the corresponding MMs. For Ag, Al, Pt, and Pd the ZGNR is relatively closer to the substrate with correspondingly vanishing MMs. This implies that the MMs are sensitive to the influence of the substrate even when the interaction between the metal and ZGNR is relatively weak. In real experimental situations, whether the MMs vanish or not also depends on other structural details such as the presence of impurities, defects, and the exact binding sites.[21] Investigating all of these structural details is beyond the scope of this work; in the following we shall focus on the effects of an external bias voltage on the properties of the relaxed ZGNRs, since they are independent of the initial configuration of MMs.

III. BIAS VOLTAGE EFFECT

The reason why the ZGNR-metal interaction plays a crucial role in determining the MMs can be explained by the Stoner model. A freestanding ZGNR has half-filled dangling bonds at the edges which results in a sharp peak of DOS at the Fermi level. If the Stoner criterion for ferromagnetism $D(E_f)I > 1$ is satisfied, the system will be spin polarized.[22] Here $D(E_f)$ is the DOS at the Fermi level and I is the Stoner parameter describing the strength of the exchange correlation. Since the DOS peak is sharp, the condition can easily be switched on/off when a gate voltage is applied which shifts the peak around the Fermi level. The metal substrate thus acts as a gate electrode when the ZGNR approaches it. When a bias voltage is applied on the system, it will either enhance or reduce the influence of the substrate and therefore can be used to tune the MMs of the ZGNR. In other words, a bias voltage can switch on/off the spin transport channel along the ZGNR edges.

Nevertheless, the substrate cannot be considered to only act as a gate. We will show that the metal substrates can be classified into two groups. One is the s-dominated metals such as Ag, Au, and Cu, for which the DOS around the Fermi level is very small and the substrate does not have a strong chemical bonding with the ZGNR. The interaction between the substrate and the ZGNR is then almost exclusively electrostatic whose main effect is to shift the Stoner peak around the Fermi level as discussed above. The second group is the p- or d-dominated metals whose electronic structures hybridize with the non-bonding π orbital of the edge C atom, resulting in the broadening or distortion of the Stoner peak. Consequently, the MMs of the ZGNR are not sensitive to the bias voltage in this case.

Let us focus on the electronic structures of the ground state first. Figure 2 plots the PDOS of the edge C atom for four different systems: freestanding ZGNR, Ag/ZGNR, Au/ZGNR, and Cu/ZGNR. In the case of the freestanding ZGNR, the PDOS shows a sharp peak at the Fermi level if the spin degree of freedom is restricted. But if the spin degree of freedom is released, the peak splits into two peaks above or below the Fermi level corresponding to different spins, respectively. For the interface with vanishing MMs

TABLE I. The local magnetic moment(per edge C atom) and the binding distance between ZGNR and metal fcc (111) surface. d_e relates to the distance between the ZGNR's edge and the metal, and d_c relates to the distance between the ZGNR's center and the metal; the combination of these two parameters describes the bending of the ribbon.

	Ag	Al	Au	Cu	Ni	Pd	Pt
Magnetic moment (μ_B)	0	0	0.07	0.08	0.06	0	0
d_e (Å)	2.90	3.05	3.27	3.58	3.55	3.17	3.14
d_c (Å)	3.02	3.30	3.50	3.60	3.59	3.22	3.24

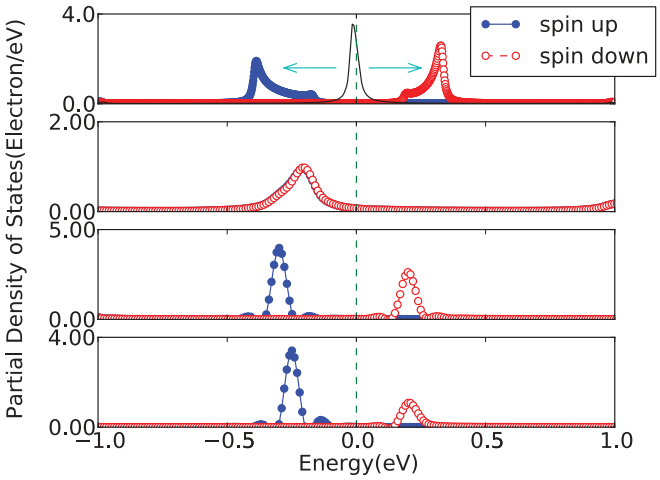

FIG. 2. (Color online) Partial density of states (PDOS) of an edge C atom at zero bias. From top down are the results of a freestanding ZGNR, Ag/ZGNR, Au/ZGNR, and Cu/ZGNR, respectively. Due to the structural symmetry, for the Ag/ZGNR case the PDOS is the same at the other edge; for freestanding, Au/ZGNR, and Cu/ZGNR cases, the curve shapes are the same while the spins are reversed. The black solid line in the upper panel represents the PDOS when the spin degree of freedom is restricted.

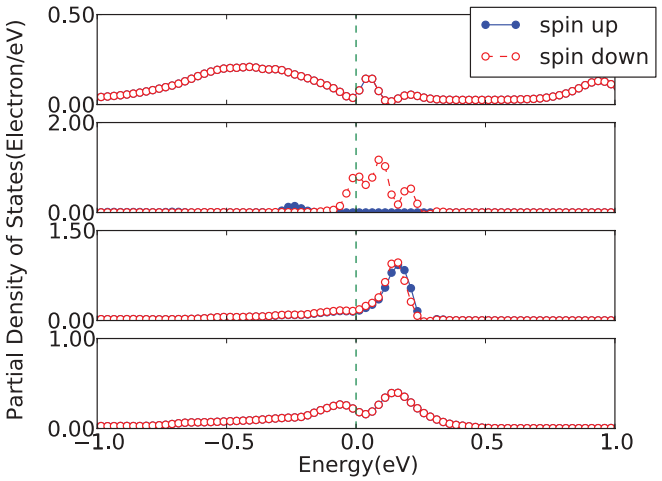

FIG. 3. (Color online) PDOS of an edge C atom at zero bias. From top bottom are results of Al/ZGNR, Ni/ZGNR, Pd/ZGNR, and Pt/ZGNR. Similar to the Ag/ZGNR case in Fig. 2, they have the same PDOSs at the other edges.

(Ag), the edge state's peak is clearly shifted away from the Fermi level. For interfaces with a finite MM (Au and Cu), the two characteristic Stoner peaks are clearly visible. Here only the PDOSs at one edge are shown and due to the structural symmetry, the PDOS is symmetric at the other edge; i.e., for Ag/ZGNR they are identical; for Au/ZGNR and Cu/ZGNR the shapes of the peaks are the same but the spins are reversed.

The behavior of the p- or d-dominated metals is more complicated as shown in Fig. 3. For p-dominated Al and d-dominated Pt, the peaks are broadened due to hybridization with the surface states of the metal and no MMs are present. Since the Ni surface is magnetic itself, after hybridization the peak is dominated by the majority spin and broadened slightly. For d-dominated Pd, the effect of hybridization is not very obvious at zero bias, but below we will see it becomes clearer at finite bias voltages. For all four systems, the PDOSs at the other edge are identical, similar to the Ag/ZGNR case in the s-metals group.

We now turn our attention to the effect of an external bias voltage on the system. The properties under an external bias voltage are calculated within the nonequilibrium Green's function (NEGF) method implemented in the GPAW code,[18,23] where the nonequilibrium electron density is calculated via the Keldysh nonequilibrium Green's functions. For detailed knowledge of this method, we refer interested readers to the original literature.[24] In the self-consistent NEGF-DFT calculations, a single-zeta-polarized (SZP) basis set is used for the metal atoms deep in the electrodes, and a double-zeta-polarized (DZP) basis is used for metal atoms in the surface layer and the C atoms in the ZGNR. One practical difficulty in the bias calculation is to avoid the situation that the self-consistent iteration falls into a trap and converges to a metastable nonmagnetic state. Since the finite bias calculation starts from the ground state which sometimes is nonmagnetic (for example, the Ag/ZGNR case), the final result will turn out to be nonmagnetic limited by the spin symmetry. To obtain the correct (energetically more stable) magnetic state, a small antiferromagnetic density should be mixed into the ground state to serve as the initial condition of the self-consistent NEGF-DFT run.

When a bias voltage V_b is applied on the junction between the metal substrate and the counter electrode, only a fraction of the voltage drops on the ZGNR due to the large vacuum barrier between the ZGNR and the counter electrode [see Fig. 1(a)]. Therefore, the energy shift in the spectrum of the ZGNR only corresponds to a fraction of the applied bias $V_{\text{shift}} = \alpha V_b$. Since α is very small ($\approx$0.02 in our calculation), a large voltage is needed in order to produce a relatively large effect. Due to the large vacuum, there is essentially no tunneling and our system is similar to a capacitor with a ZGNR in between the two capacitor plates. Note that these finite bias calculations are reasonable even at high bias because only the electrostatic response of the capacitor-like system is involved and there is no current running through the system. In the case of Ag/ZGNR, Fig. 4(a) and Fig. 4(b) show the calculated effective potential and the voltage drop along the transport direction, respectively. We can see that the potential converges to the bulk potential at 3–4 layers away from the metal surface, meaning the physical properties near the boundary are smooth and the high bias calculation is reliable.

The Ag/ZGNR system is a good example to show that the bias voltage can open the spin channels. In Fig. 4(c), we can see the band structures of the ZGNR at zero bias and at a finite bias of $V_b = 12$ V. Both band structures are spin degenerate

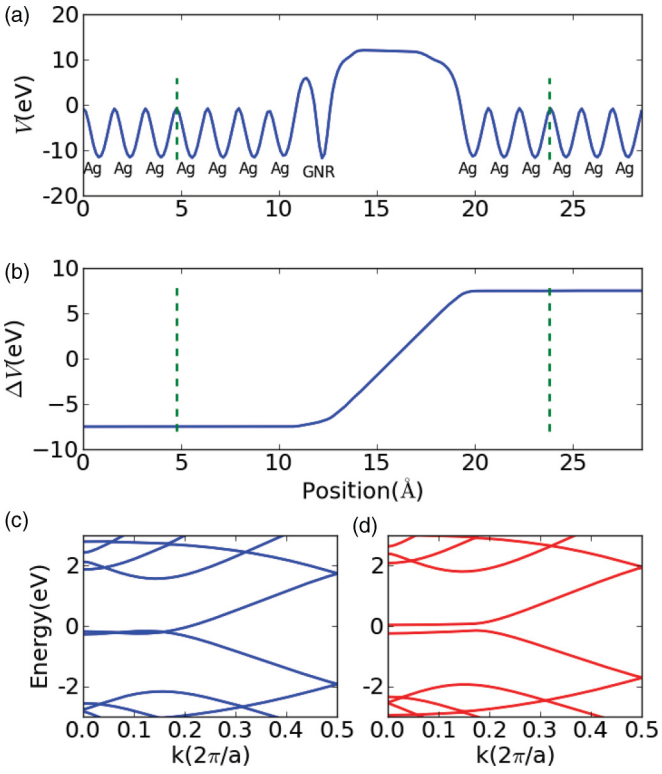

FIG. 4. (Color online) (a) The average effective potential along the transport direction for the Ag/ZGNR system. (b) The difference between the potentials at zero bias and a finite bias voltage $V_b = 15$ V. The green dashed lines represent the boundary between the bulk electrodes and the central scattering region. (c) and (d) The band structures of the Ag/ZGNR at zero bias (c) and a finite bias voltage $V_b = 12$ V (d).

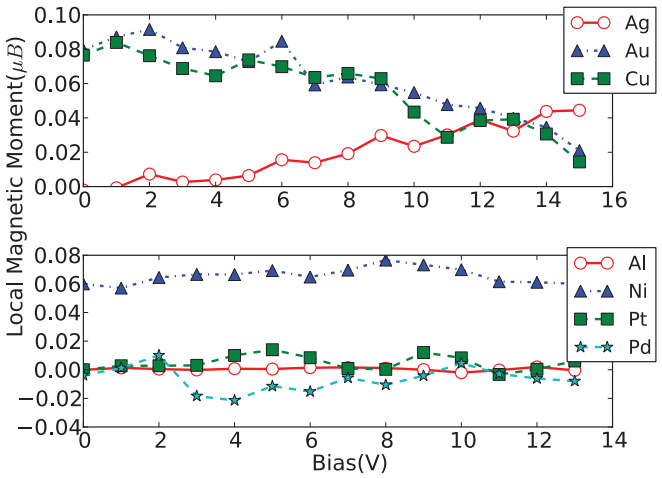

FIG. 5. (Color online) The local MM per C atom against the bias voltage on the s-dominated systems (upper panel) and the p- or d-dominated systems (lower panel).

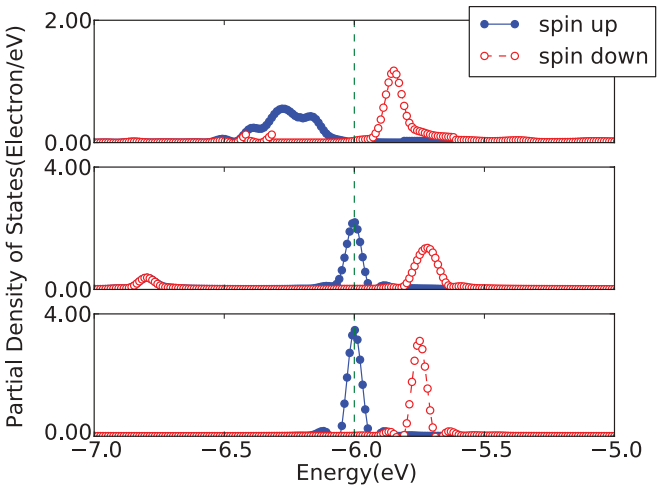

FIG. 6. (Color online) PDOS of an edge C atom at a finite bias voltage $V_b = 12$ V. The dashed green line represents the Fermi level of the left electrode. From top down are the results of Ag/ZGNR, Au/ZGNR, and Cu/ZGNR.

because of the antiferromagnetic symmetry. In the former, the horizontal line (k from 0 to 0.2) representing the edge states is shifted slightly below the Fermi level due to the interaction with the substrate, consistent with the PDOS result presented above. A gap of about 0.2 eV is opened when a 12 V bias voltage is applied. These band structures are unfolded since the unit cell in our calculations is double the size of that of the primitive ZGNR. The opening of the band gap implies that the spin channels are switched on since the conduction and valence bands are spin polarized at the edges.

After demonstrating the electric switching of the spin channels in the above specific example, we now provide an overall physical picture of the phenomena. The systematic effect of the bias voltage can be illustrated by a relationship between the bias voltages and the local MMs, as showed in Fig. 5. For the s-dominated metals, as expected, the MMs increase or decrease as a function of the bias voltage. In the case of Ag, the MM increases as a result of the shift of the occupied peak towards the Fermi level. In the cases of Cu and Au, which are initially spin polarized, the applied bias moves the peaks away from the Fermi level, thus reducing the MMs. They all roughly follow a linear trend against the bias voltage. For p- or d-dominated metals, the MMs seem to only have a small random fluctuation during the process, and the simple electrostatic interpretation is not sufficient due to the stronger hybridization between the ZGNR and the metal surfaces.

Now we examine the detailed PDOS of the ZGNR after turning on the bias voltage. In the biased situation, there are two Fermi levels in the system corresponding to the two electrodes;[23] in the corresponding plots we only show the Fermi level of the left electrode (the substrate) since the ZGNR sits on the left electrode and is strongly coupled to it. For s-dominated metal substrates, the PDOS of the edge C atom under the bias voltage $V_b = 12$ V is shown in Fig. 6. For Ag, the original nonmagnetic PDOS peak splits into two Stoner-type peaks, one residing above and the other below the Fermi level, implying that the system becomes magnetic. For the Au and Cu substrates, the gaps between the two Stoner peaks shrink and the occupied Stoner peaks start to move across the Fermi level, implying that the local MMs decrease. Clearly, it is the electrostatic effect that dominates the s-metal cases.

The results of the p and d metals are shown in Fig. 7. We can see that under a finite bias voltage, the PDOS peaks are strongly distorted and/or broadened in all the cases, indicating that states of the ZGNR hybridize with the states of the metal substrate. The PDOS peak in the Al case becomes rather smooth over a wide energy region, while for the d metals there are still some features around the Fermi level although the shapes are completely different from the ground state. In the case of Ni, some minority states mix in while the MM is not changed very much. The peaks in the Pd and Pt cases are relatively narrow in the ground state but are extended significantly under the finite bias. Thus we can conclude in these cases that the original edge states are no longer *local* and the MMs become strongly dependent on the particular electronic structure of the substrate metal. The

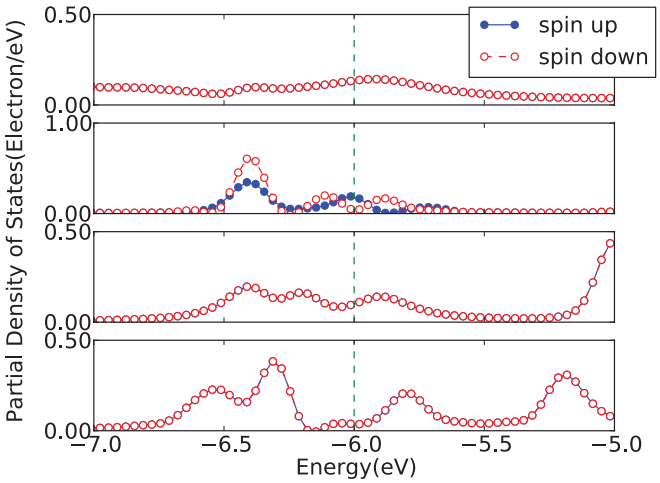

FIG. 7. (Color online) PDOS of an edge C atom at a finite bias voltage $V_b = 12$ V. The dashed green line represents the Fermi level of the left electrode. From top down are the results of Al/ZGNR, Ni/ZGNR, Pd/ZGNR, and Pt/ZGNR.

further knowledge of the nonequilibrium states under strong hybridization remains unknown and may be interesting for future work.

IV. DISCUSSION

So far we have investigated the effects of the metal substrates on ZGNRs and the possibility to tune the MMs by applying a bias voltage. The basic idea is to charge or discharge the ZGNR layer that moves the PDOS peak of the edge states toward or away from the Fermi level, subsequently affecting the edge magnetization. For *s*-dominated metals, the trend is predictably linear and thus the tuning can be in good control, which is ascribed to the electrostatic interaction between the ZGNR and *s* metals. Note that this effect is only related to the edge magnetic moments which is accompanied with a sharp DOS peak right at the Fermi level, and it is not likely to happen in the case of bulk magnetization since the corresponding DOS peak is much broader.

The reason why it is the electrostatic interaction between the ZGNR and *s* metals and the stronger hybridization (chemical interaction) between the ZGNR and *p* or *d* metals can be roughly explained by Table II. Due to the difference in the orbital degeneracy, the *s* metals have much smaller DOS at the Fermi level compared with the *p* or *d* metals; hence the *s* metals have a weaker hybridization with the ZGNR and the interaction is dominated electrostatically.

In our device model (see Fig. 1), the bias voltage is used to move the PDOS peak toward or away from the Fermi level, i.e., charge or discharge the ZGNR. To be consistent, we show in the plots the results of negative bias voltage—meaning the potential falls from the right to the left, which is to discharge the ZGNR or move the PDOS peak downward. The behavior of Pd/ZGNR under a positive bias voltage might be of interest since its PDOS peak is above the Fermi level. However, our results show that the MMs of Pd/ZGNR remain zero under a fairly large positive bias voltage (12 V).

In Fig. 8 we show the charge transfer for all the systems. All the curves are below the horizontal black dashed line, i.e., the line representing the neutral charge; this means that the ZGNR loses electrons to the metal substrates. In Table II we list the electron loss of the ZGNR in all the systems in the ground state. We can see that the *s* metals with smaller DOS at the Fermi level might have larger total charge transfer, which is different from the case in the previous works[25,26] where the metal adatoms are adsorped on a pure graphene flake and the charge transfer between the metal and graphene can be taken as a term to estimate the hybridization. In our model, the mismatch of DOS and charge transfer possibly implies that some low-energy electrons come into play. When a finite negative bias voltage is applied, the metal substrates drag electrons out of the ZGNR even further. The relations are quite linear, and combining with the relations between the bias voltage and the MMs, we conclude that it is a stable property which can be used in tuning the MMs and controlling the spin channels.

TABLE II. The PDOS at Fermi energy of per metal atom on the surface and the electron loss (ΔQ) of the ZGNR in each unit cell. The two numbers of Ni in PDOS represent the majority and minority spins.

	Ag	Au	Cu	Al	Ni	Pd	Pt
PDOS (e^-/eV)	0.12	0.14	0.11	0.24	3.8, 0.14	0.97	1.00
ΔQ (e^-)	0.72	0.32	0.33	0.85	0.19	0.45	0.23

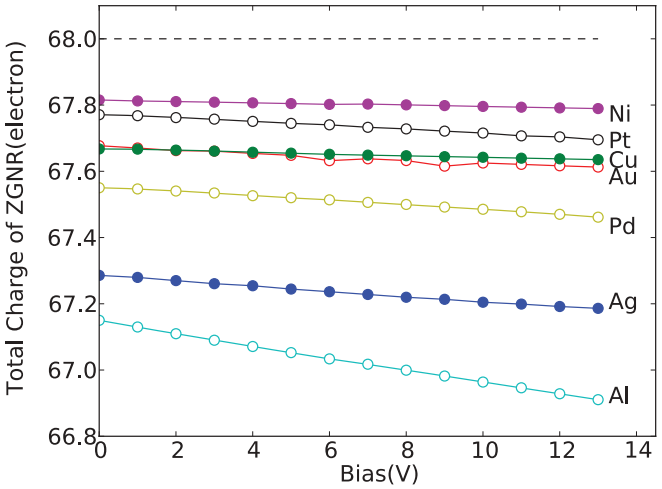

FIG. 8. (Color online) The total charge of the ZGNR in different systems under a finite bias voltage. The horizontal dashed black line represents the neutral level.

The intrinsic spin-orbit interaction (SOI) of pure graphene is extremely small and thus can be neglected. On the other hand, Nicolay *et al*. reported that the SOI is not negligible for the Au fcc (111) surface,[27] and the SOI in the combined system of Au/graphene has also been investigated.[28] Nevertheless, the tuning of edge states of the ZGNR by a bias voltage studied in this paper is mainly controlled by the electric field and the coupling strength to the substrate that is dominated by the overall DOS around the Fermi level. For the Au surface, the DOS has a very smooth *s* feature and its finer electronic structure is not expected to play any significant role.

Finally, there could be a small atomic reconstruction under finite bias. To this end we calculated the forces when increasing the bias voltage.[23] The results show that the ZGNR tends to move toward the metal substrates under a negative bias but the effect is very small: The maximum force under 12 V bias voltage is found to be only 0.03 eV/Å. This effect can also be discussed from the charge transfer point of view. The ZGNRs lose some electrons to the metal surface in equilibrium. A negative bias voltage drives slightly more electrons out of the ZGNR to the metal but this extra charge transfer is nevertheless very small—the maximum being on the order of $0.01e$ for *s* metals. The tiny charge transfer due to bias implies that the bias-induced atomic reconstruction should be very small.

V. SUMMARY

Fabrication techniques of graphene on metal surfaces have been well developed.[29] For application to nanoelectronics, one usually transfers the as-grown graphene to semiconductor surfaces for further processing. The transfer procedure has detrimental effects on the quality of the graphene. Here we found that the properties of the ZGNR on metal surfaces

have some very interesting behavior that may be exploited further. By atomistic first-principles calculations, we show that the magnetic moments are tunable by an external bias voltage applied on the *s*-metal substrates. This is due to the dominating electrostatic interaction between the ZGNR and *s*-metal surfaces. On the other hand, the ZGNR interacts strongly with *p* or *d* metals by chemical hybridization, and bias tuning is less effective. Through detailed analysis of the PDOS and charge transfer in these systems, we conclude that the Stoner effect is responsible for this phenomenon, and the process is quite linear and stable (as a function of bias), which suggests suitable applications are possible.

ACKNOWLEDGMENTS

We gratefully acknowledge financial support from NSERC of Canada, FQRNT of Quebec, and CIFAR. We thank CLUMEQ and RQCHP for providing computing facilities.

*chenj@physics.mcgill.ca

[1] Y. Kobayashi, K.-i. Fukui, T. Enoki, K. Kusakabe, and Y. Kaburagi, Phys. Rev. B **71**, 193406 (2005).
[2] Y. Kobayashi, K.-i. Fukui, T. Enoki, and K. Kusakabe, Phys. Rev. B **73**, 125415 (2006).
[3] K. Kobayashi, Phys. Rev. B **48**, 1757 (1993).
[4] K. Nakada, M. Fujita, G. Dresselhaus, and M. S. Dresselhaus, Phys. Rev. B **54**, 17954 (1996).
[5] M. Fujita, K. Wakabayashi, K. Nakada, and K. Kusakabe, J. Phys. Soc. Jpn. **65**, 1920 (1996).
[6] V. L. J. Joly, M. Kiguchi, S.-J. Hao, K. Takai, T. Enoki, R. Sumii, K. Amemiya, H. Muramatsu, T. Hayashi, Y. A. Kim *et al.*, Phys. Rev. B **81**, 245428 (2010).
[7] B. Biel, X. Blase, F. Triozon, and S. Roche, Phys. Rev. Lett. **102**, 096803 (2009).
[8] Z. Li, H. Qian, J. Wu, B.-L. Gu, and W. Duan, Phys. Rev. Lett. **100**, 206802 (2008).
[9] M. Wimmer, I. Adagideli, S. Berber, D. Tománek, and K. Richter, Phys. Rev. Lett. **100**, 177207 (2008).
[10] M. Zeng, L. Shen, M. Zhou, C. Zhang, and Y. Feng, Phys. Rev. B **83**, 115427 (2011).
[11] B. Wang, J. Wang, and H. Guo, Phys. Rev. B **79**, 165417 (2009).
[12] D. A. Areshkin and B. K. Nikolić, Phys. Rev. B **79**, 205430 (2009).
[13] M. Killi, D. Heidarian, and A. Paramekanti, New J. Phys. **13**, 053043 (2011).
[14] E. V. Castro, M. P. López-Sancho, and M. A. H. Vozmediano, New J. Phys. **11**, 095017 (2009).
[15] Z. Qiao, S. A. Yang, B. Wang, Y. Yao, and Q. Niu, Phys. Rev. B **84**, 035431 (2011).
[16] M. J. Schmidt and D. Loss, Phys. Rev. B **82**, 085422 (2010).
[17] M. Y. Han, B. Özyilmaz, Y. Zhang, and P. Kim, Phys. Rev. Lett. **98**, 206805 (2007).
[18] J. Enkovaara, C. Rostgaard, J. J. Mortensen, J. Chen, M. Dułak, L. Ferrighi, J. Gavnholt, C. Glinsvad, V. Haikola, H. A. Hansen *et al.*, J. Phys.: Condens. Matter **22**, 253202 (2010).
[19] J. P. Perdew, K. Burke, and M. Ernzerhof, Phys. Rev. Lett. **77**, 3865 (1996).
[20] M. Vanin, J. J. Mortensen, A. K. Kelkkanen, J. M. Garcia-Lastra, K. S. Thygesen, and K. W. Jacobsen, Phys. Rev. B **81**, 081408 (2010).
[21] L. R. Radovic and B. Bockrath, J. Am. Chem. Soc. **127**, 5917 (2005).
[22] See, for example, M. Peter, *Magnetism in the Solid State: An Introduction* (Springer, Berlin, 2003).
[23] J. Chen, K. S. Thygesen, and K. W. Jacobsen, Phys. Rev. B **85**, 155140 (2012).
[24] J. Taylor, H. Guo, and J. Wang, Phys. Rev. B **63**, 245407 (2001).
[25] J. Ding, Z. Qiao, W. Feng, Y. Yao, and Q. Niu, Phys. Rev. B **84**, 195444 (2011).
[26] K. T. Chan, J. B. Neaton, and M. L. Cohen, Phys. Rev. B **77**, 235430 (2008).
[27] G. Nicolay, F. Reinert, S. Hüfner, and P. Blaha, Phys. Rev. B **65**, 033407 (2001).
[28] Z. Y. Li, Z. Q. Yang, S. Qiao, J. Hu, and R. Q. Wu, J. Phys.: Condens. Matter **23**, 225502 (2011).
[29] J. Wintterlin and M.-L. Bocquet, Surf. Sci. **603**, 1841 (2009).